Heliyon 10 (2024) e24469

Contents lists available at ScienceDirect

Heliyon

journal homepage: www.cell.com/heliyon

Research article

Green^3: A green extraction of green additives for green plastics

Vera Muccilli [a,**], Anna E. Maccarronello [a], Carolle Rasoanandrasana [b], Nunzio Cardullo [a], Martina S. de Luna [d], Maria G.G. Pittalà [a], Paolo M. Riccobene [c], Sabrina C. Carroccio [c], Andrea A. Scamporrino [c,*]

[a] University of Catania – Department of Chemical Sciences, Viale A. Doria 6, 95125, Catania, CT, Italy
[b] Sorbonne Polytech - Bâtiment Esclangon, 4 Place Jussieu, Case Courrier 135, 75252, Paris, Cedex 05, Italy
[c] Institute for Polymers, Composites and Biomaterials CNR, Via P. Gaifami, 18, 95125, Catania, CT, Italy
[d] University of Naples Federico II - Department of Chemical Engineering, Materials and Industrial Production, DICMaPI, P. le Tecchio 80, 80125, Naples, Italy

ARTICLE INFO

Keywords:
Walnut shells
Agricultural waste
UV protection
Microwave-assisted extraction
Polyphenols
Response surface methodology

ABSTRACT

PLA/PBAT bioplastic is a commercial biodegradable plastic employed for packaging and several food and agriculture applications. In this regard, properties such as the antioxidant ability to extend food shelf life and light resistance, are of great interest in the production of packaging and mulching films, respectively. These features are obtained by developing blends with pure chemicals and/or natural products as additives. In the present work blend formulations of PLA/PBAT with a walnut shell extract rich in antioxidants were developed and evaluated for their properties in comparison with classic PLA/PBAT. Specifically, natural additives, and most importantly the production process were purposely selected to i) be green and cost-effective; ii) confer antioxidant properties; and iii) improve material performance.

To this aim, a walnut shell extract (EWS) with high antioxidant activity was obtained thanks to a novel green and cost-effective microwave-assisted extraction (MAE) procedure. A response surface methodology was utilized to explore how the total phenolic content (TPC) and antioxidant activity are influenced by varying aqueous ethanol concentration, extraction time, and microwave power. The highest predicted TPC and antioxidant activity were achieved when employing the ideal conditions for Microwave-Assisted Extraction (MAE): using a mixture of 30 % ethanol in water, an irradiation time of 120 s, and a microwave power of 670 W. The optimized EWS was characterized by HPLC-MS determining qualitative and quantitative data with the identification of flavonoids, fatty acids, and anacardic acids among the main components, responsible for antioxidant activity. The resulting EWS powder was melt-mixed at 140C° and 20 RPM with the bio-based PLA/PBAT bioplastic at two different concentrations (0.5 and 1.5 w/w) by forming film specimens. All EWS-based bioplastic films showed increased antioxidant features determined by the DPPH bleaching test, TEAC, and ORAC assays. The films keep the antioxidant capacity even after 7 days of UV-accelerated aging. Remarkably, adding 1.5 % EWS boosted the bioplastic UV light resistance, reducing the abatement of molecular masses by more than 60 % without affecting mechanical properties.

* Corresponding author.
** Corresponding author.
E-mail addresses: v.muccilli@unict.it (V. Muccilli), andreaantonio.scamporrino@cnr.it (A.A. Scamporrino).

https://doi.org/10.1016/j.heliyon.2024.e24469
Received 28 September 2023; Received in revised form 8 January 2024; Accepted 9 January 2024
Available online 12 January 2024

1. Introduction

Walnut shells (Juglans regia L.), accounting for a large part of the total weight of the walnut, are treated as waste for the ostensible low economic value, generally employed as fuel for domestic heating. Additional uses of the shells are proposed but of little economic impact [1]: abrasives for cleaning and polishing plastics, soft metals, stone, wood, and fiberglass; filtration media for both separating raw oils and heavy metals from water and for treating wastewater from the petrochemical industry.

In recent years, there has been a growing attention on extracting bioactive compounds, such as polyphenols, from various parts of the nut. Among these, walnut shells subjected to extraction with both lipophilic and hydrophilic extraction media proved to be a source of value-added compounds belonging to the classes of terpenes, fatty acids, and polyphenols [2]. The hydroalcoholic extracts from walnut shells have even higher phenolic content and antioxidant activity than walnut kernel and fruits. In particular, taxifolin, gallocatechin, gallic acid, and tyrosol are the most abundant phenolics identified in walnut shell extracts with antioxidant activity [2].

Recently, other shells as by-products from the agrifood industry, namely almond and pistachio hard shells [3,4], were extracted with alcoholic solutions to yield antioxidant constituents, including tannins, flavonoid glycosides, and phenolic acids derivatives. In a similar work, carried out on hazelnut skin by-product, several natural deep eutectic solvents (NADES) were investigated to optimize the extraction of bioactive compounds, highlighting the use of bio-renewable DES to recover natural antioxidants from hazelnut by-products [5]. Though the chemical composition of walnuts and other shells is still little investigated, is clear that this waste could be a promising feedstock for biologically active compounds, thus for preparing food additives with antioxidant and antimicrobial activity, as well as for food packaging and pharmaceutical applications. One of the main challenges in a zero-waste circular economy is the recovery of natural antioxidants from agri-food wastes and the application of "green" extraction procedures employing reduced extraction times, thus limiting the degradation of the bioactive constituents [6].

Microwave extraction (MAE) effectively satisfies these desirable requirements and was specifically chosen for this study. However, the extraction is greatly affected by time, solvents, and microwave power. Therefore, the Design of Experiment (DOE) was selected to assess how various factors impact the extraction procedure and consequently influence the outcomes of this process [7]. DOE offers benefits such as identifying the optimal response within the design matrix and elucidating the interactions among different factors. Response Surface Methodology (RSM) serves as an efficient tool that utilizes DOE to forecast the conditions resulting in the best possible response. Consequently, RSM process proves to be fast, allowing the optimization with a limited number of experiments or simulations [8]. In this study, the interplay between three factors—ethanol concentration, irradiation time, and microwave power—was analyzed using 3-D response surface plots for each dependent variable, including total phenolic content measured by TPC assay and antioxidant activity assessed by TEAC, DPPH, and ORAC assays.

Moreover, this study aims to demonstrate the real ability of optimized extract from walnut shells (EWS) to work as a UV stabilizer and antioxidant agent for bioplastic formulations.

Specifically, in view of an entirely eco-sustainable approach to designing new composites and blends, the EWS was directly added to PLA/PBAT bioplastic as an additive to improve the polymer's behavior in terms of UV resistance, without affecting the mechanical properties of the material. In this scenario, careful consideration is essential when assessing the incorporation of fillers into the matrix. Indeed, despite the improvement of the target properties, the risk of influencing the mechanical stability could be high. PLA/PBAT bioplastic is a commercial biodegradable plastic produced by BASF that covers packaging and agriculture applications [9]. This bioplastic is a mixture of 84 % poly (butylene adipate-*co*-terephthalate) (PBAT), 4 % polylactide acid (PLA), and 12 % of inert additives [10].

In this regard, properties such as the antioxidant ability to extend food shelf life [11], and light resistance, are of great interest in producing packaging and mulching films, respectively.

It is worth noticing that, the literature reports several notable papers on the use of natural molecules as potential antioxidants and/or stabilizers for plastics [12–14]. However, most of them proposed a "model approach" in which the obtained positive results are related to the addition of pure active molecules to the plastic samples [14–18]. The proposed approaches could be far from some industrial requirements such as the overall reduction of cost in terms of additives production, management of waste products and purification streams, time, and energy consumption [19,20]. Noteworthy, from the eco-sustainable point of view, the inevitable purification steps needed to obtain pure molecules, can thwart the effort in replacing synthetic additives with natural ones. With this regard, the use of extracts, rich in antioxidant compounds, obtained from agri-food wastes, is a challenge for the study and realization of new bioplastics for industrial purposes, reducing the costs relative to the use of pure compounds.

Recently, Li et al. showed that cardanol-loaded halloysite added to PLA improved its long-term thermo-oxidative resistance and crystallization property (owing to the stabilizing properties of cardanol [18]. P. Scarfato et al. demonstrated the ability of hazelnut perisperm to provide antioxidant properties to PLA/PBAT bioplastic films making them sealable in a wide range of temperatures [11]. In a different study, films made from composite PLA/PBAT-grapefruit seed extract demonstrated excellent UV-light blocking abilities and strong antibacterial effects against Listeria monocytogenes [21]. Considering these outcomes, and the poor searches in the use of antioxidants from biowastes for the formulation of new bioplastic blends, EWS was included in the PLA/PBAT blend formulation and tested as follows reported.

2. Experimental

2.1. Chemicals and reagents

All chemicals were of reagent grade and were used without further purification; Folin–Ciocalteau, 2,4,6-tri (2-pyridyl)-1,3,5-triazine, 2,2-diphenyl-1-picrylhydrazyl radical (DPPH•), formic acid (FA), fluorescein, quercetin, gallic acid, potassium persulfate ($K_2S_2O_8$), 6-hydroxy-2,5,7,8-tetramethylchroman-2-carboxylic acid (Trolox®), 2,2′-Azino-bis(3-ethylbenzothiazoline-6-sulfonic acid) diammonium salt (ABTS), tetrahydrofuran (THF) were bought from Merck (Darmstadt, Germany). The 2,2′-Azobis (2-methyl-propionamidine) dihydrochloride (AAPH) was purchased from Acros Organics. Sodium carbonate (Na_2CO_3), HPLC grade water, and acetonitrile (ACN) were bought from Carlo Erba (Milan, Italy). Analytical standards quercetin-3-*O*-glucoside and (17:1)-anacardic acid were bought from Merck (Darmstadt, Germany); stearic acid was bought from Carlo Erba (Milan). Ecovio® F23B1 bio-based and biodegradable PLA/PBAT pellets were purchased by BASF SE Global Marketing Biopolymers (Ludwigshafen Germany). They were used after an overnight stay in a vacuum oven at 50 °C.

2.2. Plant material

Walnuts (Juglans regia L.) harvested in October 2021 were furnished by a local farmer in Milo (Catania, Italy). Cleaned shells were dried at room temperature, and ground in an electrical grinder (KYG model-CG9430, 300 W). The ground powders were passed through a 1 mm sieve used to ensure the homogeneity of the residue powders, then collected in vacuum packaged in PET bags and stored at −20 °C until further use.

2.3. Microwave-assisted extraction (MAE)

The extraction from walnut shell samples was performed on a domestic microwave oven (Smeg S43 Type F322EC). The apparatus consists of a digital control system for setting microwave power (linearly adjustable from 150 to 1000 W) and extraction time and. The oven was modified with a hole on the top (18 mm diameter) and a chilled water system to condense the vapours produced during the extraction.

The walnut shell samples (3.0 g) were extracted using aqueous ethanol as solvent at a solid-to-solvent ratio of 1:10 (w/v). The ethanol concentration, microwave power and extraction time were varied according to the experimental design reported in Table A. The extractions reported in Table A were carried out in sealed vessels, and no evaporation was observed. Following Microwave-Assisted Extraction (MAE), the extracts underwent filtration using a Buchner funnel lined with Whatman No.1 filter paper. The resulting supernatants were gathered and then dried until reaching a constant weight. During the extractions performed in optimal condition, the temperature of the samples at the end of extraction never exceeded 54 °C. The extracts were stored in a freezer (−20 °C) until their use.

To evaluate the feasibility of a possible scale-up of the extraction protocols proposed in this study, extraction was performed onto a glass bulb connected to the chilled water system. Walnut powder (58 g) was suspended in 580 mL of hydroalcoholic solution and extracted under the optimized MAE conditions (62 % EtOH, 670 W and 120 s). The extract was filtered under vacuum and dried to constant weight.

2.4. Total phenolics content (TPC) quantification

The TPC of extracts was evaluated by the Folin–Ciocalteu assay, as already reported [3]. Briefly, samples were solubilized at a concentration of 10 mg/mL and diluted to 0.5 mg/mL. Distilled water (75 μL) was pipetted in each well; then samples were added (25 μL) followed by Folin–Ciocalteu's reagent previously diluted in water (25 μL). The plate was shaken at 25 °C for 6 min. Lastly, 100 μL of a 1.9 M Na_2CO_3 solution were added. The plate was put again under stirring for 1 min and incubated at room temperature for 1 h and 30 min, protected from light. Subsequently, the optical density was measured at 765 nm using the Synergy H1 microplate reader (BioTek, Bad Friedrichshall, Germany) equipped with Gen5 software.

Gallic acid served as the standard and underwent the same protocol as the other samples. A 1 mg/mL stock solution of gallic acid was prepared and diluted in aliquots (25, 50, 100, 200, and 400 μL) to produce the calibration curve. Results, obtained in quadruplicate and reported as mean ± SD, were calculated as mg of gallic acid equivalents per g of extract (mg GAE/g). Afterward, considering the extraction yields, these units were converted to mg GAE/g of dried walnut shells starting material (mg GAE/g dw), considering the yield of each extract effectively obtained.

2.5. Evaluation of the antioxidant activity

2.5.1. Oxygen radical absorbance capacity (ORAC) of extracts

The ORAC of the extracts was determined according to a previously reported method [22]. A stock solution of fluorescein (0.54 mM) was prepared by dissolving 7.5 mg of fluorescein in a mixture of 50:50 PB S (50 mM; pH 7.4): EtOH; a diluted solution (8.16 × 10–5 mM) was freshly prepared in PBS before the assay. Concisely, buffer (for blank; 25 μL), sample solutions from extracts (0.05 mg/mL; 25 μL), Trolox (5–40 μM; 25 μL) or quercetin (2.5 mM; 25 μL) were pipetted in 96-well-microplate, followed by the addition of fluorescein (8.16×10^{-5} mM in PBS; 150 μL). The microplate was incubated at 37 °C for 10 min. Finally, AAPH (0.153 mM; 25 μL) was

pipetted and the fluorescence was immediately acquired every 1 min for 30 min, setting excitation at λEx = 485 nm and emission at λEm = 528 nm. The ORAC values were obtained from the elaboration of the area under the curve (AUC) by linear regression (R^2 = 0.9993) with Trolox results. The final data (as mean ± SD; n = 4) of extracts were expressed as μmol of Trolox equivalents per g of dried extract (μmol TE/g), considering the yield of each extract effectively obtained.

For all the samples and the standard, the antioxidant capacity was calculated according to equation (1):

$$ORAC = \frac{\left(AUC_{sample} - AUC_{blank}\right)}{\left(slope\ AUC_{Trolox}\right)} \times \frac{1}{\left(\frac{g}{L} sample\right)} \quad (1)$$

2.5.2. DPPH• radical scavenging activity of extracts

The electron donation ability of the extracts was measured by bleaching the purple-coloured solution of DPPH•. This solution, freshly prepared (190 μM in methanol; 200 μL), was mixed with 10, 20, 40, 60 μL 20 μL of extract samples (0.5 mg/mL) or standard (quercetin, 0.05 mg/mL) and the mixture was incubated at 25 °C for 1 h in the dark.

The optical density of the mixture (ODsample) was acquired at 515 nm with Agilent BioTek Synergy H1 Multimode Reader using the Gen5 software. For each group of samples, a blank was prepared by employing MeOH or EtOH in place of samples (these solutions are employed to determine the ODcontrol). DPPH•/methanol solution was used as a blank.

For all the samples and the standard, the yield of the % of quenched DPPH was determined according to equation (2).

$$quenched\ DPPH\cdot\ \% = \frac{\left(OD_{control} - OD_{sample}\right)}{OD_{control}} \times 100 \quad (2)$$

The results of the extracts were expressed as mg of Trolox equivalents per gram of starting material (mg TE/g dw), by means of a calibration curve obtained with Trolox (0–0.8 mM; R^2 = 0.9997).

2.5.3. Trolox equivalent antioxidant capacity by ABTS•+ assay (TEAC) of extracts

The ABTS•+ stock solution was prepared as previously reported [3]. A working solution (70 μM) was obtained by dilution with EtOH, and pipetted (200 μL) in each well after the addition of sample solution (0.05 mg/mL; 10, 20 or 30 μL). The plate was stirred at 23 °C for 6 min, and the OD at 734 nm was read. The % of quenched ABTS•+ was obtained by equation (3). The obtained results were analyzed using linear regression based on the standard curve of trolox. (obtained in the range 5–40 μM; R2 = 0.9991) and are expressed as mg of Trolox equivalent antioxidant capacity (TEAC) per gram of walnut shells starting material (mg TE/g dw).

$$quenched\ ABTS^{\cdot+}\ \% = \frac{\left(OD_{blank} - OD_{sample}\right)}{OD_{blank}} \times 100 \quad (3)$$

2.5.4. Antioxidant activity of PLA/PBAT film films

ORAC assay. Samples of films **1**–**4** and **1a**-**3a** were suspended in EtOH (concentration ranging from 40 to 20 mg/mL). The mixtures were sonicated (Bandelin sonorex; 480 W, 35 kHz) at 27 °C for 30 min. Then the mixtures were incubated for 24 h at 25 °C. For ORAC assay a fluorescein working solution (8.16 × 10–5 mM; 150 μL) was shaken with 20 μL of extracted samples in a black 96-well microplate at 37 °C for 10 min. Subsequently, a 153 mM AAPH solution (25 μL) was introduced, and the fluorescence intensity was monitored using the specified parameters: λEx = 485 nm, λEm = 528 nm, gain 50, for 30 min at 1-min intervals. The data were processed using equation (1), and the outcomes were reported as μmol TE/g of film.

DPPH• assay. Samples of the obtained films **1**–**4** and **1a**-**3a** were weighted (6.8–2.1 mg) and extracted with EtOH (150 μL) by sonication (Bandelin sonorex; 480 W, 35 kHz) at 27 °C for 30 min. Afterward, the plate was kept in an incubator at 25 °C for a duration of 24 h. The resulting solutions were mixed and incubated with a 0.38 mM DPPH solution (150 μL) at 25 °C. After 2 h, the solutions were moved to 96 well-microplate plate and OD was recorded at 510 nm with Sinergy H1 plate reader. Results were elaborated as mgTE/g of film referring to a calibration curve (R^2 = 0.9991) obtained testing trolox standard solutions (0.01–0.2 mg/mL) and plotting the % of quenched DPPH vs Trolox concentration. For all the samples and the standard, the yield the % of quenched DPPH was determined according to equation (2).

The percentage of radical scavenging activity (RSA%) obtained at 10 mg/mL was also reported in Table 5.

TEAC assay by ABTS. For the assay the same mixtures of **1**–**4** and **1a**-**3a** prepared for ORAC were employed. A 70 μM ABTS•+ was added (200 μL) to each well where aliquots of extracts (20 μL) were previously inserted. The mixtures were agitated at 23 °C for 6 min, following which the optical density at 734 nm was measured. The data were elaborated as Trolox equivalents antioxidant capacity (TEAC) per gram of film (μmol TE/g) referring to a calibration curve (R^2 = 0.9979) obtained testing trolox standard solutions (40–350 μM) in the same conditions of the samples. For all the samples and the standard, the % of quenched ABTS•+ was determined according to equation (3).

All assays were performed in triplicate. Student's *t*-test was used to determine the significant difference of the antioxidant.

2.6. Experimental design and statistical analysis

Response surface methodology (RSM) with a three-factorial Box-Behnken experimental design (BBD) was adopted to evaluate the effects of operating extraction variables (X1 – X3) on the TPC and antioxidant activity (measured with DPPH•, ORAC, and TEAC

assays) of Juglans regia L. shell extract. The developed models were used to assess the impacts of individual factors and their interactions, enabling the determination of the most favorable extraction conditions for achieving the highest recovery of polyphenols exhibiting antioxidant properties from walnut hard shells.

The experimental design was generated using JMP® statistical software (SAS Institute S. r.l., Milano, Italy). Equation (4) was derived from mathematical models based on a 15-run experimental setup, incorporating three replicates at the central point (as outlined in Table 1):

$$N = 2k\ (k-1) + C_o \tag{4}$$

in this equation, k represents the number of factors, and C0 denotes the count of central points. Three levels of factors were coded as −1 (low), 0 (midpoint), and +1 (high), as detailed in Table 1. To mitigate the impact of systematic errors on the observed response, all experiments were conducted randomly.

The response surfaces of the dependent variables TPC (Y1), ORAC (Y2), DPPH• (Y3), and TEAC (Y4) underwent a natural logarithmic transformation and were accommodated by a second-order polynomial model, as expressed in Equation (5):

$$Y = B_0 + \sum_{i=1}^{k} B_i X_i + \sum_{i=1}^{k} B_{ii} X^2 + \sum_{i>j}^{k} B_{ij} X_i X_j + E \tag{5}$$

where Y represents the predicted response; X represents the independent variable; B0 is a constant coefficient; Bi, Bii, and Bij are the linear, quadratic, and interactive regression coefficients, respectively. The assessment of model adequacy included examining the lack of fit, the coefficient of determination (R2), and the F-test value derived from the analysis of variance (ANOVA). Regression analysis and three-dimensional response surface plots were generated to ascertain the ideal conditions for maximizing TPC and antioxidant activity. Statistical significance testing relied on the total error criteria with a confidence level of 95 %.

Experimental measurements were plotted on Excel 16 and reported as mean ± standard deviation of four measurements. All the obtained data were compared by one-way ANOVA using OriginPro 2021 software. A p-value threshold of 0.05 was considered statistically significant according to Tukey's test.

2.7. HPLC-MS analysis

Mass spectrometric (ESI-MS/MS) analysis was carried out on an ion trap mass spectrometer equipped with an ESI ion source (LTQ, Thermo Fischer Scientific, San Jose, CA, USA). The mass spectrometer was coupled online with an LC pump (Dionex Ultimate 3000, Thermo Fischer Scientific, San Jose, CA, USA). The optimized extract was dissolved in a 50:50 mixture of MeOH and H2O at a concentration of 50 mg/mL. Then, 20 μL of the sample was loaded onto a Waters Symmetry RP-C18 column (150 mm × 1 mm i. d., 100 Å, 3.5 μm), using the autosampler, and the column was maintained at 25 °C.The elution was conducted at a rate of 50 μL/min using a gradient of H_2O + 1 % FA (solvent A) and ACN + 1 % FA (solvent B) as follows: at t0 min, B (5 %); at t25 min, B (15 %); at t40 min, B (25 %); at t55 min, B (55 %); at t60 min, B (95 %); at t65 min, B (100 %); and finally at t80 min, B (5 %). Full scan mass spectra were acquired in negative ionization mode in the *m/z* range 150–2000. ESI ion source operated with 220 °C capillary temperature, 30 a. u.

Table 1
Experimental design and results in terms of TPC and radical scavenging activity for Juglans regia L. hard shells.

Run	Independent variables			Dependent variables			
	MAE conditions			Experimental measures			
	X_1 (MW, W)	X_2 (EtOH, %)	X_3 (Time, s)	Y_1, TPC[1] (mg GAE/g dw)	Y_2, ORAC[2] (μmol TE/g)	Y_3, DPPH (mg TE/g dw)	Y_4, TEAC (mg TE/g dw)
1	670	30	90	7.87 ± 1.68^{abc}	605.94 ± 41.7^{a}	1.60 ± 0.65^{ab}	2.16 ± 0.75^{abc}
2	1000	30	90	5.94 ± 1.55^{defg}	438.03 ± 19.0^{cdef}	1.34 ± 1.82^{abc}	1.78 ± 0.39^{cd}
3	670	90	90	5.33 ± 1.38^{efg}	393.14 ± 30.1^{ef}	0.63 ± 0.39^{def}	0.81 ± 1.23^{f}
4	1000	90	90	5.16 ± 1.21^{fg}	380.82 ± 10.7^{ef}	0.77 ± 0.11^{cdef}	0.96 ± 0.66^{ef}
5	670	60	60	7.36 ± 1.54^{abcd}	542.55 ± 32.6^{abcd}	1.43 ± 0.73^{abc}	1.92 ± 0.18^{bcd}
6	1000	60	60	5.83 ± 1.39^{efg}	430.10 ± 11.3^{def}	1.10 ± 1.29^{bcdef}	1.33 ± 0.45^{def}
7	670	60	120	7.99 ± 0.71^{ab}	589.01 ± 51.2^{ab}	1.44 ± 1.91^{abc}	2.51 ± 1.03^{ab}
8	1000	60	120	7.43 ± 1.08^{abc}	547.11 ± 30.7^{abc}	1.37 ± 1.26^{abc}	1.87 ± 0.24^{bcd}
9	850	30	60	5.65 ± 1.26^{efg}	408.15 ± 32.4^{ef}	1.26 ± 1.95^{bcde}	1.64 ± 0.43^{cde}
10	850	90	60	6.51 ± 0.78^{cdef}	482.02 ± 42.1^{bcde}	0.61 ± 1.74^{ef}	0.81 ± 0.52^{f}
11	850	30	120	8.36 ± 1.76^{a}	615.91 ± 36.8^{a}	2.00 ± 0.82^{a}	2.64 ± 0.77^{a}
12	850	90	120	4.98 ± 1.02^{g}	365.76 ± 20.2^{f}	0.55 ± 0.78^{f}	0.71 ± 0.67^{f}
13	850	60	90	6.43 ± 1.23^{cdefg}	477.23 ± 34.8^{cde}	1.32 ± 1.56^{abc}	1.71 ± 1.33^{cd}
14	1000	90	120	5.51 ± 1.67^{efg}	406.80 ± 61.1^{ef}	0.53 ± 0.34^{f}	0.83 ± 0.92^{f}
15	850	60	90	6.67 ± 0.94^{bcde}	444.42 ± 12.7^{cdef}	1.33 ± 0.57^{abc}	1.83 ± 0.97^{cd}

[1]Total phenolic content (TPC): results are presented as equivalent of gallic acid (GAE) in mg/g of dried starting material, expressed as mean ± SD (n = 4). [2]Oxygen Radical Absorbance Capacity (ORAC). [3]TEAC assay using ABTS. All antioxidant activity results are depicted as Trolox equivalent (TE) of dried walnut shell starting material, displayed as mean ± SD (n = 4). Dissimilar letters within the same column signify significant differences (Tukey's test $p < 0.05$).

Sheath gas, 4 kV source voltage and −18 V capillary voltage. The data-dependent method was used for mass spectrometric analysis, employing a normalized collision energy of 29 a. u. And setting the activation Q at 0.250. Mass calibration was conducted using a standard mixture comprising caffeine (Mr 194.1 Da), MRFA peptide (Mr 524.6 Da), and Ultramark (Mr 1621 Da). Data acquisition and analyses were carried out utilizing Xcalibur v. 1.3 Software (Thermo Fischer Scientific, San Jose, CA, USA).

2.8. Blend preparation

After permanence in a vacuum oven at 50 °C, the extract and the polymer were physically mixed respecting the percentages shown in Table 5. The materials were stored in the vacuum oven until the processing.

2.9. Film preparation

Specimens were prepared by hot press forming process. Specifically, the polymer was put in a Brabender's chamber at a temperature of 140 °C. The polymer was introduced in small aliquots, in the time window of 1 min, under a screws rotation rate of 20 RPM. When melted, the polymer was processed for 5 min. The melt was recovered and split into two aliquots of 10 g each. After that, the material was subjected to molding pressure through a hydraulic press PM20 by Campana S. r.l. Milano, Italy at 140 °C and 5 bar. After 5 min, the plates were rapidly cooled keeping the pressure constant. Two films having a thickness of 32.2 ± 3 μm were produced for each sample.

2.10. Methods of analysis

2.10.1. Differential scanning calorimetry (DSC)

DSC analyses were performed through a Q100 DSC calorimeter (TA Instruments, New Castle, Delaware, US). The reliability of the analyses was verified by performing the calibration by evaluating the melt purity of Indium Standards (156,6 °C and 28.45 J/g).

Each sample was subjected to a heating ramp (10 °C/min) from 20 °C to 200 °C, followed by a quenching (rate 50 °C/min) to −80 °C. The samples were brought back to 200 °C via a second heating ramp (10 °C/min). Fig. S2 shows the thermograms referring to the second heating ramp of Sample1, 2, and 3.

2.10.2. Thermogravimetric analysis (TGA)

Weight Loss Analyses were performed on ca 5 mg of each sample using a TGA Q500 (TA Instruments, New Castle, Delaware, US). The nitrogen flow during the analyses was set at 60 mL/min; the temperature range investigated was 50–800 °C, at a heating rate of 10 °C/min.

2.10.3. Size exclusion chromatography (SEC)

All the analyses were carried out through an AZURA® SEC Lab system (KnauerWissenschaftliche Geräte GmbH, Hegauer Weg, 38, 14,163 Berlin, Germany), equipped with 1 TS K gel Guard Super H–H column (3 μm, 4.6 × 35 mm) and 3 columns TSK gel connected in series and a RI detector.

2.10.4. UV light aging

All film samples were subjected to UV light irradiation up to 7 days by using a QUV Panel apparatus. The aging chamber is equipped with UV lamps with a maximum of 340 nm operating with an irradiance of 0.68 W/cm × nm at 60 °C. At least three films for each sample were exposed.

2.10.5. Mechanical characterization

The tensile properties were estimated at room temperature and humidity using an Instron machine (Tensometer 2020, Alpha Technologies) according to ASTM test method D882. Pristine and UV-irradiated films were tested at 10 mm min^{-1} until break. The Young's modulus (E), tensile strength (σ_{max}) and elongation at break (ε_{break}) were recorded. The data reported are average values.

3. Results and discussion

3.1. Model fitting

In this study, the effects of microwave (MW) power (X_1), ethanol concentration (X_2), and extraction time (X_3) were evaluated with the Box–Behnken experimental design (BBD) for MAE extraction of walnut hard shells. As is known polar organic solvents such as methanol and ethanol (EtOH) are the most effective in the recovery of (poly)phenolic compounds, among these, ethanols is GRAS and commonly employed in industrial preparations for food and pharmaceutical applications. Thus, EtOH was chosen extractive solvent together with water. The data for Total Phenolic Content (TPC) and antioxidant activity, evaluated through ORAC, DPPH, and TEAC assays from 15 experimental runs employing MAE, were subjected to ANOVA analysis, as presented in Table 1. These results were listed concerning the starting material (hard shells), in agreement with previous studies on similar waste biomasses [4,23]. The TPC ranged from 4.98 to 8.36 mg GAE/g dw, whereas for the antioxidant capacity, the ORAC values ranged from 365.75 to 615.90 μmol TE/g, the DPPH values from 0.53 to 2 mg TE/g dw, and the TEAC values from 0.71 to 2.64 mg TE/g dw. The quality of the fitted models

can be determined by the coefficients of correlation (R^2), which were $R^2 = 0.98$ for TPC and ORAC, $R^2 = 0.97$ for DPPH, and $R^2 = 0.96$ for TEAC. The adjusted determination coefficients (Adj. R^2) were 0.96, 0.94, 0.93, and 0.90 for TPC, ORAC, DPPH, and TEAC, respectively (Table S2). The coefficients being near 1 suggest a strong correlation between the observed and predicted values. The relationship between actual (experimental data) and predicted values is shown in Fig. S1. Additionally, the low coefficient of variation (CV = 1.43 %) signified a high level of precision and reliability in the experimental values [24]. The adequate precision, measuring the signal-to-noise (S/N) ratio, was higher than 4 for all the models (Table S2), indicating the models' appropriateness to navigate the experimental space [25].

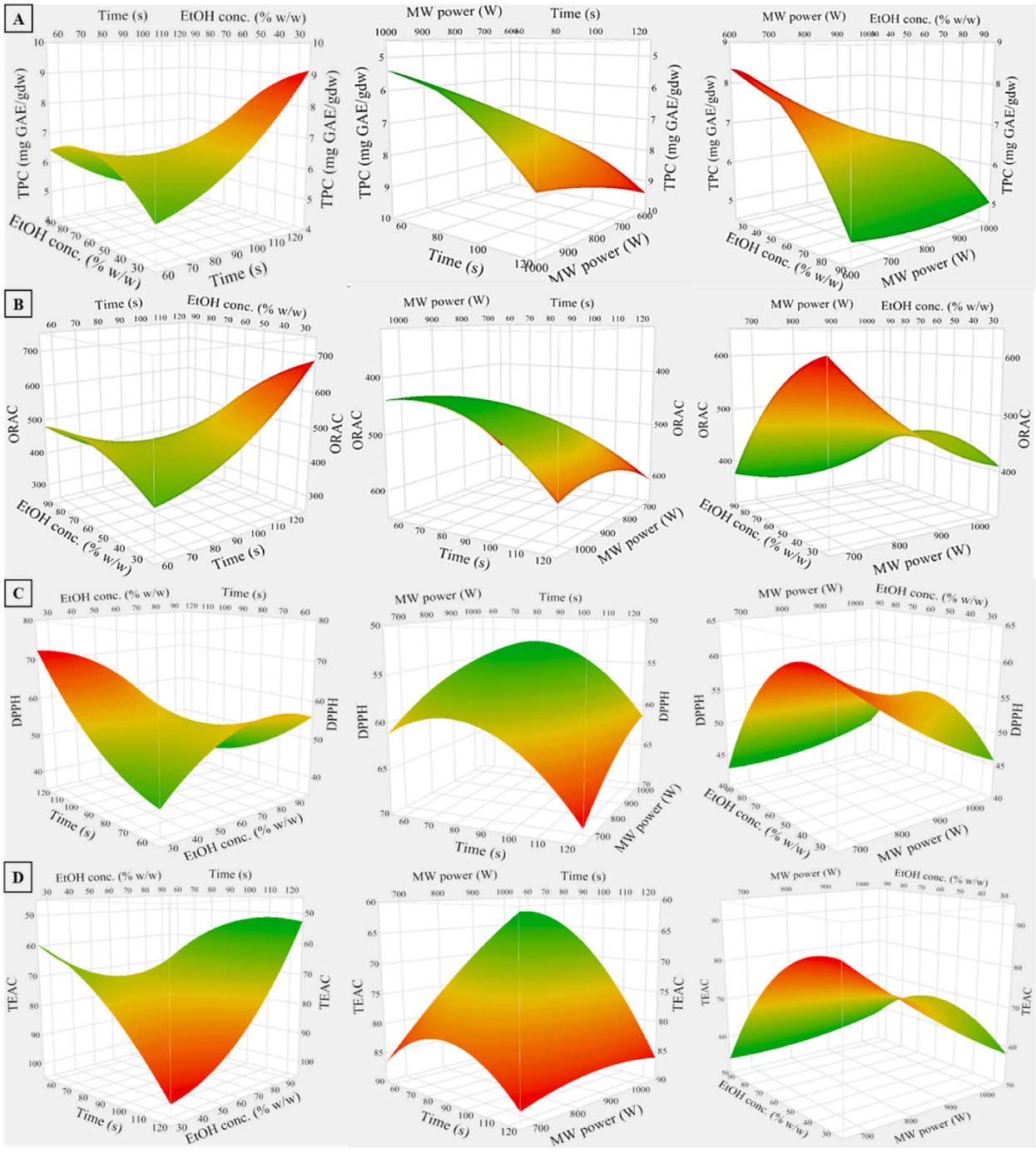

Fig. 1. Response surface 3D plots for the effect of the independent variables of ethanol concentration, extraction time and microwave power on the dependent variables TPC (A), ORAC (B), DPPH (C) and TEAC (D).

A quadratic equation was applied to the gathered data to assess the significance and adequacy of the model. The obtained p-values for both the Total Phenolic Content (TPC) and antioxidant activity confirmed the model's capability to accurately predict responses. The regression coefficients of the model's intercept, linear, quadratic and interaction terms were calculated using the least squares technique, as shown in Tables S1 and S2 of Supporting materials. The p-value of the model was less than 0.05 for all the considered responses, which indicates that the model adequately explained the responses observed about the phenolic content and antioxidant activity of walnut hard shells.

Table S2 shows the ANOVA results with the contribution of each factor under study. The greater the absolute F-value, the more significant the corresponding variables. The F-value of the model was 42.29 for TPC, whereas concerning the free radical scavenging activity, the F-value of the model was 29.83 for ORAC, 23.24 for DPPH, and 16.97 for TEAC.

Moreover, all examined operational parameters (X1 – X3) notably impacted ($p < 0.05$) both the Total Phenolic Content (TPC) and the antioxidant activity of the extract. However, the model highlighted that the most significant linear variable for TPC, ORAC, DPPH, and TEAC was the ethanol concentration, with respective F-values of 102.70 ($p < 0.0001$), 74.50 ($p < 0.0001$), 146.38 ($p < 0.0001$), and 91.41 ($p < 0.0001$). That is, the increment of phenolic content and antioxidant activity depended mostly on ethanol concentration.

Moreover, the interaction between the solvent concentration and the irradiation time (X_2X_3) was found to be highly significant ($p < 0.05$) for the ORAC, the DPPH, and the TEAC values. On the opposite, the interaction between the microwave power and the extraction time (X_1X_3) was found to have no significant effects on the antioxidant activity.

Lastly, the fitting of each model was also evaluated by the lack of fit, which was insignificant for TPC (0.2160) and antioxidant activity (0.4384, 0.2811, and 0.2848 for ORAC, DPPH, and TEAC, respectively), indicating the goodness of the model (Table S2).

Based on these findings, the model proved suitable for predicting TPC, ORAC, DPPH, and TEAC due to the high R^2 values, significant p-values, and the lack of significant p-values for the lack of fit. The final second-order polynomial equations, illustrating the empirical relationships between the responses (Y1 – Y4) and the extraction operating conditions (X1 – X3), are provided below:

$$Y_1(TPC) = 16.2798 - 0.0203x_1 + 0.0821x_2 - 0.0509x_3 + 4.11 \times 10^{-6}x_1^2 - 6.89 \times 10^{-4}x_2^2$$

$$+ 5.08 \times 10^{-4}x_3^2 + 9.51 \times 10^{-5}x_1x_2 + 5.11 \times 10^{-5}x_1x_3 - 0.0012x_2x_3$$

$$Y_2(ORAC) = 1684.0462 - 2.4341x_1 + 3.7378x_2 - 4.4265x_3 + 8.25 \times 10^{-4}x_1^2 - 0.0369x_2^2$$

$$+ 0.0439x_3^2 + 0.0082x_1x_2 + 0.0035x_1x_3 - 0.0893x_2x_3$$

$$Y_3(DPPH) = 2.2659 - 0.0031x_1 + 0.0221x_2 + 0.0040x_3 + 4.99 \times 10^{-7}x_1^2 - 2.61 \times 10^{-4}x_2^2$$

$$+ 1.55\times10^{-5}x_3^2 + 10.23\times10^{-5}x_1x_2 + 0.0035x_1x_3 - 2.09 \times 10^{-4}x_2x_3$$

$$Y_4(TEAC) = 4.8341 - 0.0077x_1 + 0.0233x_2 + 0.0047x_3 + 2.38 \times 10^{-6}x_1^2 + 3.67 \times 10^{-4}x_2^2$$

$$+ 8.68\times10^{-5}x_3^2 + 3.15\times10^{-5}x_1x_2 + 6.84\times10^{-6}x_1x_3 - 3.07 \times 10^{-4}x_2x_3$$

The results obtained from the optimization analysis using RSM for the evaluation of the effect of extraction parameters demonstrated the achievement of a reliable mathematical model that could be applied for the maximum recovery of TPC and antioxidants from walnut shells.

3.2. Response surface analysis of total phenolic content (TPC) and antioxidant activity

The response surface analysis allows for the observation of the correlation between the independent and dependent variables incorporated within the model. 3D-response surface plots, based on the model equations mentioned above, make it easier to visualize the mutual effects between two factors and how the responses are influenced by their interaction [26].

Fig. 1 shows the effects of paired independent variables on TPC (Fig. 1A), ORAC (Fig. 1B), DPPH (Fig. 1C), and TEAC (Fig. 1D). In general, all four response variables exhibited comparable behavior in their respective response surface profiles. Fig. 1A shows that when the ethanol in water concentration was fixed at 30 %, the extraction of phenolic compounds showed a slight increase with longer extraction times, reaching its peak at 120 s. Moreover, the interaction between MW power and ethanol concentration (X_1X_2), as well as between MW power and extraction time (X_1X_3), showed that the highest TPC yield could be obtained by using low MW powers (600–700 W). Farid Dahmoune et al. noted a comparable trend in their observations for the MAE of polyphenols from Myrtus communis L. leaves, probably due to the thermal degradation of phenolic compounds occurring at higher MW powers [27]. Fig. 1B to D depict the combined influence of microwave power and irradiation time on the antioxidant activity assessed by ORAC, DPPH, and TEAC. Overall, as the microwave power and extraction time (X_1X_3) decreased to 600 W and 120 s, respectively, the values of all dependent variables exhibited an increase. Regarding the interaction between microwave power and ethanol concentration (Fig. 1B to D), it is notable that higher antioxidant capacity values were evident at lower microwave power settings (600–700 W) and an ethanol concentration around 30 %.

3.3. Walnut shells extraction: model validation

Based on the RSM predictive models and values shown in Fig. 1, the ideal MAE conditions for maximum TPC recovery from walnut hard shells were estimated to be: 30 % for the ethanol concentration, 120 s for the irradiation time, and 670 W for the microwave power. Thus, according to the polynomial equations obtained, optimal conditions were: for ORAC = 34 %, 114 s, and 670 W; for DPPH = 30 %, 120 s, 670 W; for TEAC = 37.8 %, 118 s, 681 W.

Hence, it was concluded that the optimal experimental conditions to have an extract from walnut hard shells with maximum recovery of polyphenols and with the highest antioxidant activity were: EtOH: 30 % in water, irradiation time 120 s and microwave power 670 W. Under these optimized conditions, the expected values are: TPC (8.43 < 8.92<9.42 mg GAE/g_{dw}, ORAC (644.84 < 692.5< 740.07 μmol TE/g_{dw}), DPPH (1.61 < 1.93< 2.25 mg TE/g_{dw}) and TEAC (2.68 < 3.02< 3.36 mg TE/g_{dw}), respectively. A new extraction was performed under the above-mentioned optimal conditions to validate the adequacy of the model. Predicted and experimental (n = 4) results for the optimized extract from walnut hard shells (EWS) are shown in Table 2. The experimental results were in great agreement with the predicted values, suggesting that the proposed MAE protocol can be effectively used to extract phenolic compounds from walnut hard shells. Moreover, EWS exhibited a TPC of 8.49 mg GAE/g dw of shells, which was higher than the one reported by Prgomet et al. for an almond shell extract (6.30 mg GAE/g dw) obtained by stirring [4].

In Table 2, the TPC and antioxidant activity are also referred to the dried extract instead of walnut shell powder, to compare our data with findings on similar works. Specifically, the TPC of 8.49 mg GAE/g dw corresponds to a value of 249.7 mg GAE/g of extract, which was notably higher than the one reported by Herrera et al. for the walnut shell extract (13.14 mg GAE/g of extract) obtained by accelerated solvent extraction (ASE) in water [2], suggesting that the use of hydro-alcoholic solvent allows greater extraction of phenolic compounds.

Regarding the antioxidant activity, EWS showed a DPPH value of 1.67 mg TE/g dw of extract, corresponding to 59.2 mg TE/g of shells. This outcome is higher the finding reported by Soto-Maldonado et al. with DPPH values ranging from 25 to 30 mg TE/g for walnut shells extracted by conventional solid-liquid extraction [23].

3.4. Characterization of the optimized extract from walnut shells and quantification of the main constituents

HPLC/ESI-MS/MS was performed on the extract obtained with the optimized extraction parameters (EWS) in both positive and negative ionization in order to identify the phytochemicals. However, all the identifications were tentatively obtained using the negative ionization mode. The resulting total ion current chromatogram (TIC) obtained in negative mode is reported in Fig. 2.

ESI-MS and MS/MS data were cross-referenced with relevant literature to tentatively identify each compound, as outlined below. Table 3 enumerates the identified compounds, progressively numbered according to their HPLC/ESI-MS retention times. For each compound, the [M − H]− *m/z* value is provided, alongside the primary fragments observed in the MS/MS spectrum. A total of 46 compounds were tentatively identified (Table 3) and grouped mainly in hydrolyzable tannins (**14, 15 and 20**), flavonoids (**7**, **10**–**13**, **16**, **18**), xanthones (**19**, **21**), fatty acids (**9**, **23**–**26**, **28**–**31**, **33**–**35**, **37, 38, 40**–**44**) and phenolic lipids such as anacardic acids (**31**, **35**, **38**, **44**–**46**). These two last groups encompass the most abundant components of the TIC chromatogram, with trihydroxy-octadecenoic acid isomers (**24** and **25**) eluting in the peak with the highest intensity.

In addition, other constituents including organic acids (**1**–**5**), a lignin oligomer (**22**) and a lignan (**26**) were tentatively identified as well. Despite the efforts made, three unknown compounds for which it was not possible to elucidate a structure due to a lack of sufficient evidence are included in Table 3. These latter are listed as unknowns (U1, U2 and U3).

The identification of hydrolyzable tannins (compounds 14, 15, and 20) in EWS was supported by the formation of characteristic product ions arising from the depletion of gallic acid (M − H – 170), galloyl unit (M − H – 152), as well as from the consecutive losses of gallic acid and galloyl (M − H – 170–152) [50,51].

A total of seven flavonoids were identified in EWS, including quercetin and kaempferol derivatives. Compound 7, with a [M − H]– ion at *m/z* 433, was tentatively recognized as a quercetin pentoside isomer. This conclusion was drawn from the presence of a fragment ion at *m/z* 301 (M − H – 132), signifying the loss of a pentose, and a fragment at *m/z* 271, suggesting a 3-*O*-glycosyl flavonol (M − H – CH2O) [3]. Compounds 10 to 13 exhibited product ions resulting from the loss of a hexose moiety (M − H – 162). Moreover, the MS/MS spectrum of compound 10 revealed a fragment ion at *m/z* 303, characteristic of the taxifolin aglycone, tentatively identifying it as a taxifolin 3-*O*-hexoside isomer. The MS/MS spectrum of 11 displayed a product ion at *m/z* 285, indicative of kaempferol, leading to its tentative identification as kaempferol-3-*O*-hexoside. Similarly, compound 12 was identified as quercetin-3-*O*-hexoside, owing to the presence of an intense fragment ion at *m/z* 301, corresponding to the quercetin aglycone. Additionally, peak 13, with [M−H]− at *m/z* 303, was tentatively identified as taxifolin, evidenced by diagnostic fragments at *m/z* 285 (M − H – 18, loss of H_2O) and 125 (M − H – 178) [38]. Compound 16 displayed a molecular ion at *m/z* 447 and was tentatively recognized as quercetin-*O*-rhamnoside due to

Table 2
TPC and in vitro antioxidant activity evaluation (ORAC, DPPH, and TEAC) of optimized extract from walnut hard shells (EWS). Comparison between actual-by-predicted values.

Response	Y_1, TPC (mg GAE/g_{dw})	Y_1, TPC (mg GAE/g)	Y_2, ORAC (μmol TE/g_{dw})	Y_3, DPPH (mg TE/g_{dw})	Y_3, DPPH (mg TE/g)	Y_4, TEAC (mg TE/g_{dw})	Y_4, TEAC (mg TE/g)
Observed	8.49 ± 0.94	249.7 ± 3.5	668.3 ± 30.5	1.67 ± 0.15	59.20 ± 2.6	2.88 ± 0.21	96.26 ± 0.6
Predicted	8.92 ± 0.50	278.9 ± 18.1	692.5 ± 47.6	1.93 ± 0.32	57.03 ± 3.8	3.02 ± 0.34	100.26 ± 10.3

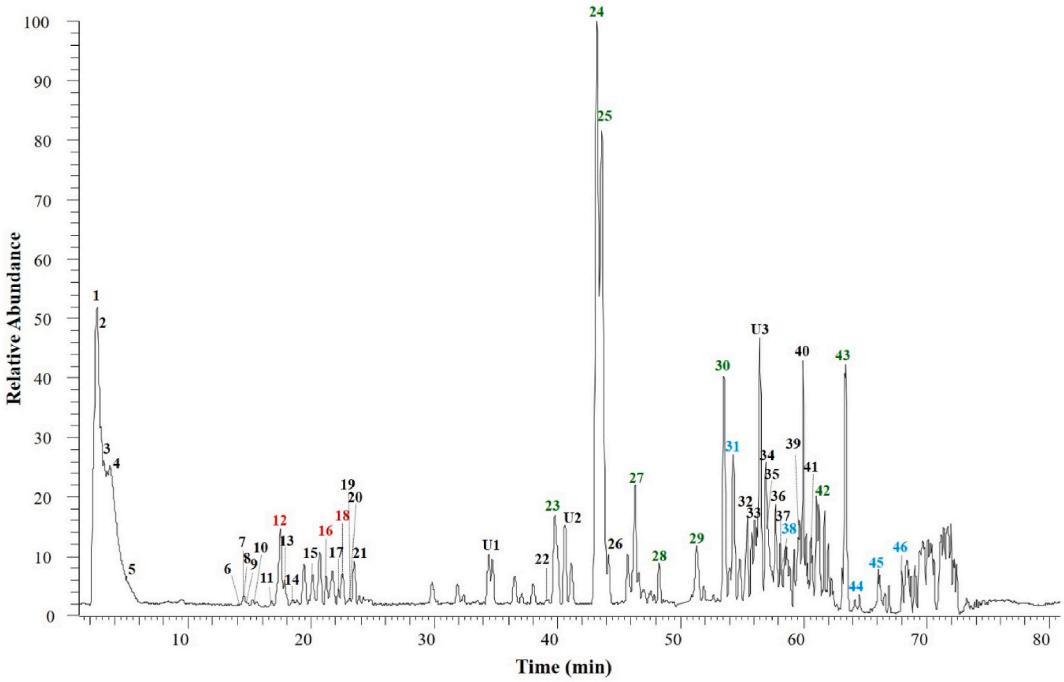

Fig. 2. HPLC/ESI-MS/MS profile of the optimized walnut hard shell extract (EWS). Peak assignments are reported in Table 3. Peaks enhanced with colours are quantified as reported in Table 4. (For interpretation of the references to colour in this figure legend, the reader is referred to the Web version of this article.)

fragment ions at *m/z* 301, resulting from the loss of a rhamnoside moiety (M − H −146), and at *m/z* 300, corresponding to quercetin [36]. Compound 18 exhibited a molecular ion [M − H]− at *m/z* 615, along with product ions at *m/z* 301 related to quercetin, a fragment ion at *m/z* 463 resulting from the loss of a galloyl unit (M − H – 152), and at *m/z* 453, indicating the loss of a hexose. Hence, it was tentatively identified as a quercetin galloylhexoside isomer.

Tentative identifications of fatty acids were achieved by comparing the molecular masses with the information retrieved from LIPID MAPS® Structure Database (LMSD) [52]. Moreover, characteristic fragmentation patterns were observed. Peaks 23–25, 27–30 and 37, exhibiting $[M - H]^-$ ions at *m/z* = 329, 327, 313, 311 and 295, respectively, show a characteristic negative product ion at *m/z* 171, containing both a carboxyl and a hydroxyl group (–$OOC(CH_2)_7CH$–OH). Furthermore, a neutral loss of [M − H – 100] caused by the fragmentation of the end-group HO–CH═$CH(CH_2)_3CH_3$, can be observed as well [43].

A total of six anacardic acids (31, 35, 38, 44–46) with different saturation degrees and lengths of alkyl chains (C13, C15, C16 and C17) were identified in EWS. The characteristic loss of CO_2 (M − H – 44) from the phenolic carboxyl group was observed for all of them. In addition, compound 44 exhibited a daughter ion at *m/z* 107, corresponding to the loss of the phenol group [37].

Some constituents of the extract have been quantified by HPLC-MS employing as standards quercetin-3-*O*-glucoside for compound 12, 16 and 18; (17:1) anacardic acid for 23, 25, 26, 28, 29, 31, 32, 39, 43–47. The results are reported in Table 4.

3.5. Polymer formulation

The obtained extract (EWS) was used as an antioxidant additive to formulate bioplastic films. In addition, the efficacy of EWS in working as a UV light stabilizer was also investigated by measuring variation in molar mass values pre and after aging. Mechanical modules were also tested.

To this purpose, commercial PLA/PBAT blend (see experimental part) was processed in a Brabender and then molded with a hot-press obtaining two different film formulations with the 0.5 and 1.5 % w/w of EWS. Other formulations have been not studied as increasing in the % of extract worsens the mechanical modules of the film.

All PLA/PBAT films were exposed to UV accelerated aging for up to 7 days and characterized by thermal, chemical-physical, and mechanical analysis. The first two columns of Table 5, report the names and the description of formulated films. Fig. S3 (A, B, and C) shows the photo of samples 1,2 and 3 immediately after passing through a heat press for the preparation of the films. The IPCB Institute logo has been placed under each membrane to show its transparency. Fig. S4 shows the portion of each of the three samples (1,2, and 3), placed in the holders for insertion into the accelerated aging system.

Table 3
Results of the identification from HPLC/ESI-MS/MS of the main constituents within the walnut hard-shell extract (EWS).

Peak no	t_R (min)	$[M-H]^-$	MS/MS Fragments, *m/z* (Relative Intensity)	Identification	Ref.
1	2.5	133	115(100); 87(5)	malic acid	[28]
2	2.5	195	129(100), 177(40); 99(10), 75(5)	gluconic acid	[29]
3	3.6	209	191(100); 85(30); 165(30); 133(30); 173(5); 129(5)	glucaric acid	[29]
4	3.6	191	111(100); 173 (50); 127(5); 155(5)	quinic acid	[30]
5	4.6	353	191(100); 179(40); 309(20); 135(5)	neochlorogenic acid	[31]
6	14.5	447	401(100); 269(10); 161(10); 327(5)	benzyl alcohol hexose-pentose derivative (formate adduct)	[32]
7	14.5	433	301(100); 151(5); 271(5)	quercetin-3-*O*-pentoside	[3]
8	14.5	377	331(100); 179(5); 119(5)	saccharide derivative	[33]
9	14.5	333	167(100); 285(40); 165(30); 135(20); 152(10); 315(5); 271(5)	(20:5) hydroperoxyeicosapentaenoic acid isomer	[34]
10	15.2	465	447(100); 299(10); 239(10); 303(5); 285(5)	taxifolin-3-*O*-hexoside isomer	[35]
11	16.7	447	281(100); 285(40)	kaempferol-3-*O*-hexoside	[36]
12	17.5	463	301(100); 271(10)	quercetin 3-*O*-hexoside	[37]
13	17.8	303	285(100); 125(10)	taxifolin	[38]
14	18.6	787	617(100); 623(20); 465(10)	tetragalloyl hexose isomer	[3]
15	20.3	939	769(100); 787(15); 617(10); 447(5)	pentagalloyl hexose isomer	[3]
16	21.3	447	301(100); 300 (30); 302(20)	quercetin-*O*-rhamnoside	[36]
17	22.2	187	125(100); 169(20); 160(20); 97(5)	hydroxygallic acid	[39]
18	22.5	615	585(100); 597(80); 453(50); 463(20); 301(20)	quercetin galloylhexoside isomer	[3]
19	23.1	583	463(100); 301(40); 565(5); 271(5)	tetrahydroxyxanthone-di-O,C-hexoside	[40]
20	23.1	1091	–	hexagalloyl hexose isomer	[3]
21	23.4	273	255(100); 258(5)	methoxy-trihydroxyxanthone	[41]
U1	34.3	597	505(100); 553(80); 383(80); 549(30); 401(20); 357(10)	–	
22	38.1	809	791(100); 743(80); 761(70); 773(60); 713(40); 565(30); 417(15)	oligolignol G (8-*O*-4)S (8-8)S (8-*O*-4)G)	[42]
23	39.8	327	229(100); 291(80); 171(80); 211(60); 209(20)	(18:2) trihydroxy-octadecadienoic acid isomer	[43]
U2	40.6	449	403(100); 311(20); 329(15)	–	
24	43.3	329	229 (100); 211 (60); 311(40); 293(20); 171(20); 183(10)	(18:1) trihydroxy-octadecenoic acid isomer	[43]
25	43.3	329	229 (100); 211 (60); 311(40); 293(20); 171(20); 183(10)	(18:1) trihydroxy-octadecenoic acid isomer	[43]
26	44.1	375	357(100); 297(20)	7-hydroxylariciresinol isomer	[44]
27	46.3	327	309(100); 291(40); 209(20); 171(20); 163(5)	(18:2) trihydroxy-octadecadienoic acid isomer	[28]
28	48.3	329	171(100); 201(80); 229(10); 211(10); 185(5)	(18:1) trihydroxy-octadecenoic acid isomer	[45]
29	51.3	311	293(100); 275(20); 211(10); 183(10); 171(5)	(20:0) dimethyl-octadecanoic acid isomer	[28]
30	53.5	313	295(100); 277(10); 171(10); 213(5)	(18:1) octadecanoic acid isomer	[45]
31	54.3	359	341(100); 315(40); 297(30)	(16:1) anacardic acid	[37]
32	55.3	265	97 (100); 238(10)	(17:2) heptadecynoic acid isomer	
33	55.8	279	97(100); 261(10); 235(10)	(18:2) linoleic acid	[46]
U3	56.4	430	386(100); 412(60); 144(40); 368(20); 259(10);	–	
34	56.9	315	297(100); 295(20); 279(20); 199(20)	(18:0) dihydroxystearic acid isomer	[45]
35	56.9	361	317(100); 293(50)	(16:0) anacardic acid	[47]
36	57.8	309	291 (100)	(20:1) eicosenoic acid isomer	[48]
37	58.9	295	277(100); 171(60)	(18:2) octadecadienoic acid isomer	[48]
38	58.9	341	323(100); 297(60)	(15:3) anacardic acid	[37]
39	59.4	293	249(100); 97(80); 185(60); 197(20)	(19:2) octadecadienoic acid isomer	[28]
40	59.9	530	279(100); 249(40); 511(25); 267 (15)	(36:3) linolenyl oleate	[49]
41	60.7	339	183(100); 239(10); 198(100); 321(5); 99(5)	(22:0) docosanoic acid	[46]
42	61.2	337	294(100); 319(49)	(22:1) docosenoic acid	[48]
43	63.4	271	225(100); 187(10); 125(10)	(16:0) hydroxypalmitic acid isomer	[45]
44	64.5	317	273(100); 107(5)	(13:1) anacardic acid	[37]
45	66.3	345	301 (100)	(15:1) anacardic acid	[37]
46	68.1	373	329 (100)	(17:1) anacardic acid	[37]

3.6. Thermal analysis

In Fig. 3A–C was reported the TG and the DTG of the A) EWS; B) the pristine PLA/PBAT film, and C) the blend with the addition of 1.5 % of EWS.

As expected, the DTG registered for EWS consists of a multi-complex peaks profile due to the weight loss overlap of the different components constituting the extract. Up to 100 °C the EWS is stable to the temperature showing a weight loss inferior to 1.14 % of the mass. From 130° to 200 °C, the main decomposition process is most likely associated with the decarboxylation of the acidic part of EWS compounds such anacardic acids [53,54]. Indeed, it is well stated in the literature that in this range of temperature, the decomposition of anacardic acids, among the main EWS constituents, takes place by forming cardanols [55]. At higher temperatures, the maximum rate of decomposition registered at around 276 °C can be reasonably assigned to the decomposition of cardanol. The latter was produced at lower temperatures (decarboxylation step) from the anacardic acids [53,54]. In Fig. 3B the TG and DTG of PLA/PBAT film were reported. The thermal profile evidenced a shoulder at 345 °C ascribable to PLA decomposition and a temperature at a maximum

Table 4
Quantification ± standard deviation of the main constituents of walnut hard-shell extract (EWS) by HPLC/ESI-MS.

Compounds	mg/g of dw extract
Flavonoids	
quercetin-3-*O*-galactoside (12)[a]	*0.223 ± 0.014*
quercetin-*O*-rhamnoside (16)[a]	0.039 ± 0.002
quercetin galloylhexoside isomer (18)[a]	0.061 ± 0.008
Fatty acids	
(18:2) trihydroxy-octadecadienoic acid (23)[b]	0.515 ± 0.058
(18:1) trihydroxy-octadecenoic acid isomer (24, 25)[b]	4.958 ± 0.023
(18:2) trihydroxy-octadecadienoic acid isomer (27)[b]	0.463 ± 0.034
(18:1 trihydroxy-octadecenoic acid isomer (28)[b]	0.131 ± 0.018
(20:0) dimethyl-octadecanoic acid (29)	0.249 ± 0.011
(18:1) octadecanoic acid isomer (30)[b]	0.858 ± 0.026
(22:1) docosenoic acid (42)[b]	0.197 ± 0.016
(16:0) hydroxypalmitic acid (43)[b]	0.862 ± 0.027
Phenolic lipids	
(16:1) anacardic acid (31)[b]	0.436 ± 0.032
(15:3) anacardic acid (38)[b]	0.068 ± 0.009
(13:1) anacardic acid (44)[b]	0.040 ± 0.012
(15:1) anacardic acid (45)[b]	0.100 ± 0.008
(17:1) anacardic acid (46)[b]	0.077 ± 0.007

[a] Quantified as quercetin-3-*O*-glucoside.
[b] Quantified as (17:1) anacardic acid.

Table 5
Nomenclature of prepared PLA/PBAT Films and antioxidant activity of films 1 − 4 evaluated with DPPH, TEAC, and ORAC assays.

Sample	Composition	DPPH (mgTE/g)	RSA% DPPH[a]	TEAC (μmol TE/g)	ORAC (μmol TE/g)
1	Pristine PLA/PBAT	0.19 ± 0.01	2.9 ± 0.1	0.17 ± 0.05	21.7 ± 1.9
1a	aged PLA/PBAT	0.19 ± 0.04	3.4 ± 0.7	0.28 ± 0.09	28.3 ± 2.0
2	PLA/PBAT + 0.5 % EWS	1.25 ± 0.08	19.8 ± 0.8	0.76 ± 0.13	42.1 ± 2.6
2a	aged PLA/PBAT + 0.5 % EWS	0.92 ± 0.07	22.2 ± 1.0	0.71 ± 0.16	46.8 ± 1.8
3	PLA/PBAT + 1.5 % EWS	2.10 ± 0.10	29.4 ± 1.3	1.57 ± 0.11	85.4 ± 2.5
3a	aged PLA/PBAT + 1.5 % EWS	2.20 ± 0.15	29.0 ± 0.6	1.22 ± 0.31	83.1 ± 1.6
4	PLA/PBAT + 0.5 % Trolox	8.2 ± 0.8	77.3 ± 2.1	9.00 ± 0.15	165.8 ± 2.1

[a] Means (n = 3) ± SD of data acquired on 10 mg of film extracted with 1 mL of DPPH solution.

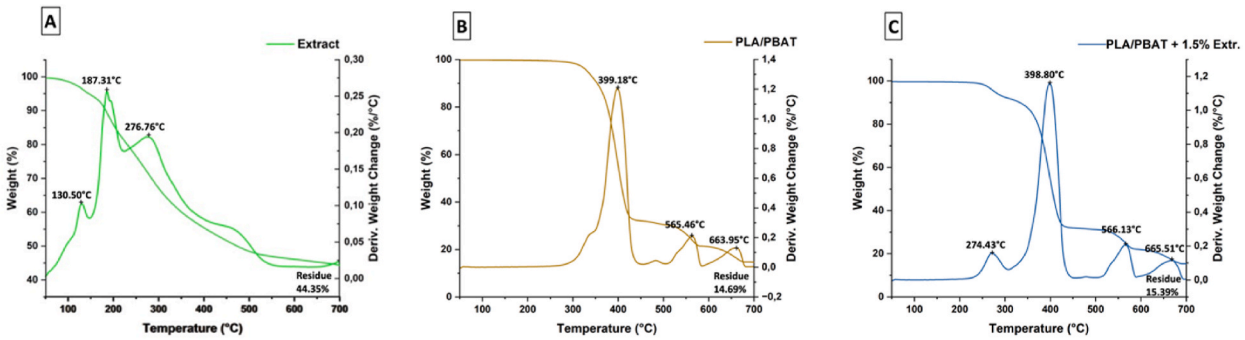

Fig. 3. TG/DTG plot of A) EWS; B) pristine PLA/PBAT, C) PLA/PBAT +1,5%$_{w/w}$ EWS.

decomposition rate of 399 °C due to the degradation of PBAT co-polyesters constituting the blend. The other degradation steps were attributed to fillers commonly added to the commercial blend. Once the EWS was added and processed at 140 °C to form films, is reasonable that the anacardic acids were readily converted into cardanols. Therefore, in Fig. 3C decomposition steps related to decarboxylation disappeared whereas it is visible at 274 °C a weight loss imputable to the presence of cardanol molecules within the blend. The residues calculation considering values of the three samples (44.3, 14.7, and 15.4, respectively) nicely confirmed the EWS weight added to the blend (1.5 % w/w), and the homogeneity of its dispersion since analysis performed in triplicate provided comparable results.

3.7. Mechanical characterization

Tensile tests were performed to investigate the effect of the extract addition on the mechanical behavior of PLA/PBAT films, as shown in Fig. 4(A-C). For pristine samples, the presence of EWS extract only has a marginal effect, with a slight reduction of the elongation at break, while Young's modulus and tensile strength are basically unaltered. Overall, we can conclude that the extract addition has no detrimental action on the mechanical performance of the polymer matrix. This is a non-trivial result, as the addition of natural extracts has been often reported to have a negative impact on the mechanical properties of polymeric films. The addition of extract powders, indeed, can be responsible for a combination of different factors, among which are the decrease of the polymer matrix crystallinity, the release of low molecular weight constituents, and stress concentration at the polymer/extract interface [11].

Focusing on the UV-irradiation aging, instead, it clearly emerges that it has a dramatic effect on the mechanical properties of the films. For the unfilled PLA/PBAT sample, Young's modulus, tensile strength, and elongation at break all were significantly reduced. In the presence of the extract, the worsening of the mechanical properties is slightly less pronounced, suggesting a possible stabilization action of the extract powders towards UV-induced aging of the polymer. To get more accurate information about this aspect, SEC analyses were carried out.

3.8. Molar masses determination

Radical degradation processes triggered by light in polyester [56,57], determine the depletion of Molar Masses (MMs) due to

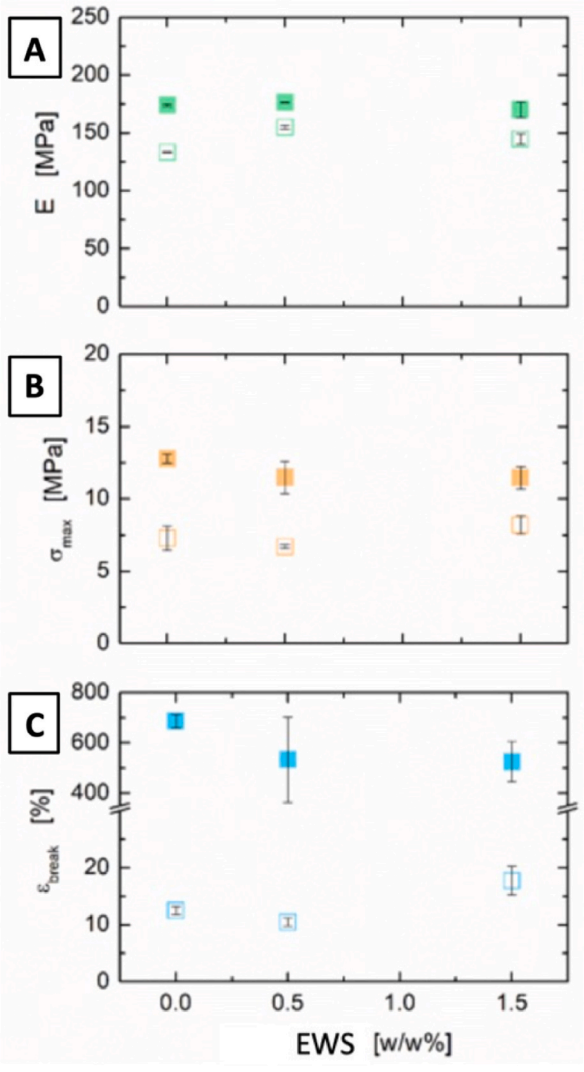

Fig. 4. Tensile properties of pristine (full symbols) and UV-irradiated (empty symbols) films of PLA/PBAT with different content of EWS: A) Young's modulus, B) tensile strength, and C) elongation at break.

random chains scission mechanisms. This undesirable process is generally avoided by adding stabilizers that protect the polymer backbones from radical attack. In this view, the efficiency of EWS in working as a polymer stabilizer can be measured by evaluating the MMs changes achieved after materials' UV exposure. For this purpose, all samples were analyzed by SEC analysis. In Fig. 5 were reported the SEC profiles of each sample typology, pre (**1**, **2**, **3**) and after aging (**1a**, **2a**, **3a**). Fig. 5A revealed that light exposure drastically affected the material with a reduction of Mw of about 52 % after seven days. Conversely, EWS preserved the blend from the radical chains scission as visible from data reported in Fig. 5B and C. Remarkably, sample 3a containing 1.5 % of EWS displayed a reduction of only 20 %. It is worth noticing that PLA/PBAT blend utilized in this work is a commercial sample that already includes a UV stabilizer in its formulation. Nevertheless, the resistance of the virgin sample to the accelerated aging results to be very poor.

3.9. Antioxidant activity of optimized walnut shell extract-loaded films

To assess the antioxidant activity of the different films (**1**–**3** and **1a** – **3a**), preliminary antioxidant tests (ORAC, DPPH and TEAC determined with ABTS) were applied to Ecovio + 0.5 % Trolox (**4**). Trolox has been used as a reference standard for these antioxidant activity assays. The results are reported in Table 5. It is worth noticing that PLA/PBAT film showed slight antioxidant activity, most likely due to the presence of light stabilizers as additives. Nevertheless, an increase of one order of magnitude (DPPH test) was measured by adding 0.5 % of EWS.

All the films loaded with EWS show valuable antioxidant activity with results ranging from 0.92 to 2.20 mg TE/g for DPPH-based assay, 0.71–1.57 μmol TE/g for TEAC (ABTS-based assay), and 42.1–85.4 μmol TE/g for ORAC. Indeed, the values are consistent with those obtained for optimized EWS (Table 2) tacking into account the amounts (0.5 and 1.5 %) loaded into the films. In detail, the antioxidant activity is higher for samples **3** and **3a** with respect to the corresponding **2** and **2a** as a consequence of the increasing amount of walnut shell extract. In fact, as clearly highlighted in Table 5, the percentage of radical DPPH quenched (RSA%) increases from 19.8 % (sample **2**) to 29.4 % (sample **3**). Furthermore, these data were comparable with those obtained by Scarfato et al. for Ecovio-haxelnut perisperm composites for active packaging application [11]. In particular, the Ecovio loaded with 1.5 % of EWS (sample 3: RSA% 29.4 %) is promising as that obtained from Scarfato et al. including 10 % of hazelnut perisperm extract and even better than composites obtained with 5 %.

Moreover, all samples **2a** and **3a**, resulting from the aging process of the corresponding samples **2** and **3,** show comparable antioxidant activity if compared to the original samples. This trend is exhibited for all couples of samples (non-aged/aged), and is in agreement with the three assays reported in Table 5. It is reasonable to suppose that for both pre-existing antioxidant and EWS formulations, molecules are well embedded within the polymeric matrix. When heated at 60 °C during UV exposure, glass transition of PLA portion occurs (Fig. S2 reporting DSC profiles). Thus, the segmental chains mobility of the material increases, allowing the segregation phase of additives at surfaces.

This phenomenon was confirmed by simply heating the pristine PLA/PBAT film (sample **1**) at 60 °C in an oven and measuring the antioxidant activity (Table S3). With a higher number of additives at the surfaces, the antioxidant activity registered for sample **1** increased. By switching on the light, the UV stabilizers work as sacrificial molecules slowing down the radical attack. As a result, the polymer will be protected from degradation. In the meantime, the antioxidant activity of stabilizers dropped down along with the exposure times, reaching the value observed in Table 5. It is worth noticing that high values measured for samples **2** and **3** endured for the aged ones **2a** and **3a** denoting that UV exposure did not affect the antioxidant performances of the natural extract within the biobased polymer blend.

4. Conclusions

Herein described the optimization of bioactive phytochemical extraction from walnut shells with a green and cost-effective method. The method performed using microwaves and a mixture of water and ethanol was selected to be oriented toward the environmental and economic sustainability of the production process. Employing a mathematical model allowed us to obtain an extract with high antioxidant activity. The direct applicability of the produced extract was proven by using it as an antioxidant and UV stabilizer additive for bioplastic material. To this purpose, extract characterized by a mix of flavonoids, fatty acids, and anacardic acids was added at different percentages by melt mixing to a biodegradable blend (PLA/PBAT) used for packaging and agriculture purposes. The formulated materials, tested by verified by TEAC, DPPH, and ORAC assays, showed remarkable antioxidant properties. Photodegradation tests on formulated blends were also performed to assess the ability of the extract as a UV stabilizer. ASTM method D882 was exploited to verify the tensile behaviors of the materials before and after UV aging, whereas SEC was used to determine the molecular masses (Mn, Mw) of the blends. The comparison of the obtained data with the reference one confirmed the improved resistance of the EWS-added PLA/PBAT. Finally, to increase the polymer durability, without impacting the mechanical properties, the maximum percentage of extract to be added has been identified as 1.5 %. More specifically, the specimen with 1.5 % of EWS underwent a reduction of the molecular masses of only 20 %, an excellent result considering the 60 % reduction of PLA/PBAT without additives. These results make the new PLA/PBAT-EWS blended films promising for further studies, including the evaluation of antibacterial activity in the preparation of industrial film packaging. As a next step of this work, eco-friendly natural deep eutectic solvents could be evaluated for new green extraction of antioxidants from walnut shells considering their potential as a source of bioactive compounds. Once the production method of the composite films is defined, LCA studies will be carried out to precisely evaluate the actual environmental impact of the proposed system.

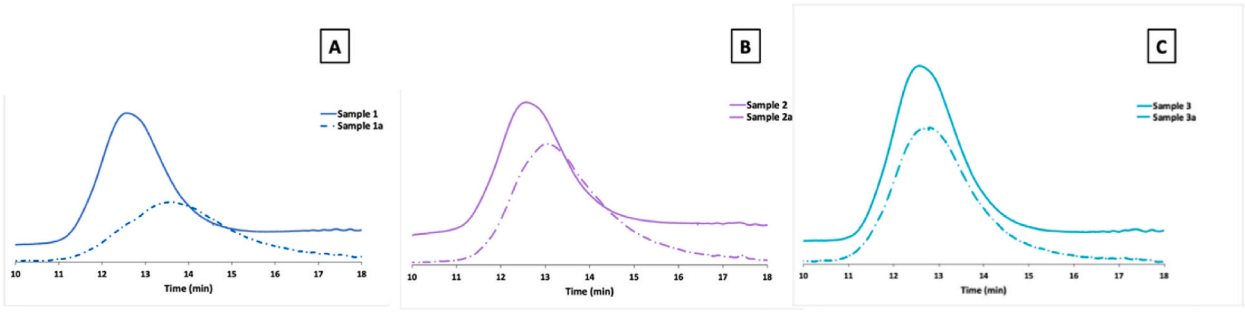

Sample	Mn	Mw	PD*	Δ% Mw
Sample 1	66.222	103.605	1.56	
Sample 1a	19.140	49.965	2.61	51.77

Sample	Mn	Mw	PD*	Δ% Mw
Sample 2	66.205	104.162	1.57	
Sample 2a	26.414	62.466	2.36	40.03

Sample	Mn	Mw	PD*	Δ% Mw
Sample 3	65.825	103.596	1,57	
Sample 3a	40.888	83.217	2.03	19.67

Fig. 5. SEC profiles and related molar masses distributions of samples: A) **1** and **1a**; B) **2** and **2a**; C) **3** and **3a**.

Funding

This work was supported by H2020-EU.3.2.1.2 project "Plastic in Agricultural Production: Impacts, Lifecycles and Long-term Sustainability—PAPILLONS" grant agreement ID: 101000210.

Data availability statement

The data associated with this study have been NOT deposited into a publicly available repository.

CRediT authorship contribution statement

Vera Muccilli: Writing – review & editing, Writing – original draft, Validation, Supervision, Funding acquisition, Conceptualization. **Anna E. Maccarronello:** Formal analysis. **Carolle Rasoanandrasana:** Investigation, Formal analysis. **Nunzio Cardullo:** Validation, Investigation, Formal analysis, Data curation. **Martina S. de Luna:** Writing – review & editing, Validation, Methodology. **Maria G.G. Pittalà:** Formal analysis. **Paolo M. Riccobene:** Investigation, Formal analysis. **Sabrina C. Carroccio:** Writing – review & editing, Writing – original draft, Validation, Supervision, Funding acquisition, Conceptualization. **Andrea A. Scamporrino:** Writing – review & editing, Writing – original draft, Validation, Supervision, Data curation, Conceptualization.

Declaration of competing interest

The authors declare that they have no known competing financial interests or personal relationships that could have appeared to influence the work reported in this paper.

Acknowledgements

The authors gratefully acknowledge the Bio-Nanotech Research and Innovation Tower of the University of Catania (BRIT; project PONa3_00136) financed by the Italian Ministry for Education, University and Research MIUR, for making available the Synergy H1 microplate reader.

Appendix A. Supplementary data

Supplementary data to this article can be found online at https://doi.org/10.1016/j.heliyon.2024.e24469.

References

[1] A. Jahanban-Esfahlan, A. Ostadrahimi, M. Tabibiazar, R. Amarowicz, A comparative review on the extraction, antioxidant content and antioxidant potential of different parts of walnut (*Juglans regia* L.) fruit and tree, Molecules 24 (11) (2019), https://doi.org/10.3390/molecules24112133.
[2] R. Herrera, J. Hemming, A. Smeds, O. Gordobil, S. Willför, J. Labidi, Recovery of bioactive compounds from hazelnuts and walnuts shells: quantitative-qualitative analysis and chromatographic purification, Biomolecules 10 (10) (2020), https://doi.org/10.3390/biom10101363.
[3] N. Cardullo, M. Leanza, V. Muccilli, C. Tringali, Valorization of agri-food waste from pistachio hard shells: extraction of polyphenols as natural antioxidants, Resources-Basel. 10 (5) (2021), https://doi.org/10.3390/resources10050045.
[4] I. Prgomet, B. Gonçalves, R. Domínguez-Perles, N. Pascual-Seva, A. Barros, A box-behnken design for optimal extraction of phenolics from almond by-products, Food Anal. Methods 12 (9) (2019) 2009–2024, https://doi.org/10.1007/s12161-019-01540-5.

[5] C. Fanali, V. Gallo, S. Della Posta, L. Dugo, L. Mazzeo, M. Cocchi, et al., Choline chloride-lactic acid-based NADES as an extraction medium in a response surface methodology-optimized method for the extraction of phenolic compounds from hazelnut skin, Molecules 26 (9) (2021), https://doi.org/10.3390/molecules26092652.

[6] A. Galuszka, Z. Migaszewski, J. Namiesnik, The 12 principles of green analytical chemistry and the significance mnemonic of green analytical practices, Trends Anal. Chem. 50 (2013) 78–84, https://doi.org/10.1016/j.trac.2013.04.010.

[7] A. Weremfo, S. Abassah-Oppong, F. Adulley, K. Dabie, S. Seidu-Larry, Response surface methodology as a tool to optimize the extraction of bioactive compounds from plant sources, J. Sci. Food Agric. 103 (1) (2023) 26–36, https://doi.org/10.1002/jsfa.12121.

[8] A.I. Khuri, S. Mukhopadhyay, Response surface methodology, WIREs Comput. Stat. 2 (2) (2010) 128–149.

[9] A.R.D. Costa, A. Crocitti, L.H. de Carvalho, S.C. Carroccio, P. Cerruti, G. Santagata, Properties of biodegradable films based on poly(butylene succinate) (PBS) and poly(butylene adipate-co-terephthalate) (PBAT) blends, Polymers 12 (10) (2020), https://doi.org/10.3390/polym12102317.

[10] R. Scaffaro, A. Maio, M. Gammino, F.P. La Mantia, Effect of an organoclay on the photochemical transformations of a PBAT/PLA blend and morpho-chemical features of crosslinked networks, Polym. Degrad. Stabil. 187 (2021), https://doi.org/10.1016/j.polymdegradstab.2021.109549.

[11] P. Scarfato, M.L. Graziano, A. Pietrosanto, L. Di Maio, L. Incarnato, Use of hazelnut perisperm as an antioxidant for production of sustainable biodegradable active films, Polymers 14 (19) (2022), https://doi.org/10.3390/polym14194156.

[12] M.G.A. Vieira, M.A. da Silva, L.O. dos Santos, M.M. Beppu, Natural-based plasticizers and biopolymer films: a review, Eur. Polym. J. 47 (3) (2011) 254–263, https://doi.org/10.1016/j.eurpolymj.2010.12.011.

[13] N.T. Dintcheva, G. Infurna, M. Baiamonte, F. D'Anna, Natural compounds as sustainable additives for Biopolymers, Polymers 12 (4) (2020), https://doi.org/10.3390/polym12040732.

[14] G. Gorrasi, V. Bugatti, M. Ussia, R. Mendichi, D. Zampino, C. Puglisi, et al., Halloysite nanotubes and thymol as photo protectors of biobased polyamide 11, Polym. Degrad. Stabil. 152 (2018) 43–51, https://doi.org/10.1016/j.polymdegradstab.2018.03.015.

[15] E. Darroman, N. Durand, B. Boutevin, S. Caillol, Improved cardanol derived epoxy coatings, Prog. Org. Coating 91 (2016) 9–16, https://doi.org/10.1016/j.porgcoat.2015.11.012.

[16] M.N. Siddiqui, H.H. Redhwi, I. Tsagkalias, E.C. Vouvoudi, D.S. Achilias, Development of bio-composites with enhanced antioxidant activity based on poly(lactic acid) with thymol, carvacrol, limonene, or cinnamaldehyde for active food packaging, Polymers 13 (21) (2021), https://doi.org/10.3390/polym13213652.

[17] P. Ezati, J.W. Rhim, Fabrication of quercetin-loaded biopolymer films as functional packaging materials, ACS Appl. Polym. Mater. 3 (4) (2021) 2131–2137, https://doi.org/10.1021/acsapm.1c00177.

[18] C.Y. Li, W.G. Gong, Q.M. Cao, Z.Y. Yao, X. Meng, Z. Xin, Enhancement of cardanol-loaded halloysite for the thermo-oxidative stability and crystallization property of polylactic acid, Appl. Clay Sci. (2022) 216, https://doi.org/10.1016/j.clay.2021.106357.

[19] T.D. Moshood, G. Nawanir, F. Mahmud, F. Mohamad, M.H. Ahmad, A. AbdulGhani, Sustainability of biodegradable plastics: new problem or solution to solve the global plastic pollution? Curr. Res. Green Sustain. Chem. (2022) 100273 https://doi.org/10.1016/j.crgsc.2022.100273.

[20] S.C. Carroccio, P. Scarfato, E. Bruno, P. Aprea, N.T. Dintcheva, G. Filippone, Impact of nanoparticles on the environmental sustainability of polymer nanocomposites based on bioplastics or recycled plastics-A review of life-cycle assessment studies, J. Clean. Prod. 335 (2022), https://doi.org/10.1016/j.jclepro.2021.130322.

[21] S. Shankar, J.W. Rhim, Preparation of antibacterial poly(lactide)/poly(butylene adipate-*co*-terephthalate) composite films incorporated with grapefruit seed extract, Int. J. Biol. Macromol. 120 (2018) 846–852, https://doi.org/10.1016/j.ijbiomac.2018.09.004.

[22] N. Cardullo, V. Muccilli, V. Cunsolo, C. Tringali, Mass spectrometry and ^{1}H-nmr study of *Schinopsis lorentzii* (quebracho) tannins as a source of hypoglycemic and antioxidant principles, Molecules 25 (14) (2020), https://doi.org/10.3390/molecules25143257.

[23] C. Soto-Maldonado, E. Caballero-Valdés, J. Santis-Bernal, J. Jara-Quezada, L. Fuentes-Viveros, M.E. Zúñiga-Hansen, Potential of solid wastes from the walnut industry: extraction conditions to evaluate the antioxidant and bioherbicidal activities, Electron. J. Biotechnol. 58 (2022) 25–36, https://doi.org/10.1016/j.ejbt.2022.04.005.

[24] M. Kahlaoui, S.B. Dalla Vecchia, F. Giovine, H.B. Kbaier, N. Bouzouita, L.B. Pereira, et al., Characterization of polyphenolic compounds extracted from different varieties of almond hulls (*Prunus dulcis* L.), Antioxidants 8 (12) (2019), https://doi.org/10.3390/antiox8120647.

[25] D. Pinto, E.F. Vieira, A.F. Peixoto, C. Freire, V. Freitas, P. Costa, et al., Optimizing the extraction of phenolic antioxidants from chestnut shells by subcritical water extraction using response surface methodology, Food Chem. (2021) 334, https://doi.org/10.1016/j.foodchem.2020.127521.

[26] M.A. Bezerra, R.E. Santelli, E.P. Oliveira, L.S. Villar, L.A. Escaleira, Response surface methodology (RSM) as a tool for optimization in analytical chemistry, Talanta 76 (5) (2008) 965–977, https://doi.org/10.1016/j.talanta.2008.05.019.

[27] F. Dahmoune, B. Nayak, K. Moussi, H. Remini, K. Madani, Optimization of microwave-assisted extraction of polyphenols from Myrtus communis L. leaves, Food Chem. 166 (2015) 585–595, https://doi.org/10.1016/j.foodchem.2014.06.066.

[28] H.G. Agalar, G.A. Ciftci, F. Goger, N. Kirimer, Activity guided fractionation of *Arum italicum* miller tubers and the LC/MS-MS profiles, Record Nat. Prod. 12 (1) (2018) 64–75, https://doi.org/10.25135/rnp.06.17.05.089.

[29] S.S. Li, Z.T. Lin, H.X. Jiang, L.K. Tong, H. Wang, S.Z. Chen, Rapid identification and assignation of the active ingredients in fufang banbianlian injection using HPLC-DAD-ESI-IT-TOF-MS, J. Chromatogr. Sci. 54 (7) (2016) 1225–1237, https://doi.org/10.1093/chromsci/bmw055.

[30] Y. Zhang, H. Xiong, X.F. Xu, X. Xue, M.N. Liu, S.Y. Xu, et al., Compounds identification in semen cuscutae by ultra-high-performance liquid chromatography (UPLCs) coupled to electrospray ionization mass spectrometry, Molecules 23 (5) (2018), https://doi.org/10.3390/molecules23051199.

[31] A. Medic, J. Jakopic, A. Solar, M. Hudina, R. Veberic, Walnut (*J. regia*) agro-residues as a rich source of phenolic compounds, Biology-Basel 10 (6) (2021), https://doi.org/10.3390/biology10060535.

[32] V. Spinola, E.J. Llorent-Martinez, S. Gouveia, P.C. Castilho, Myrica faya: a new source of antioxidant phytochemicals, J. Agric. Food Chem. 62 (40) (2014) 9722–9735, https://doi.org/10.1021/jf503540s.

[33] L. Molina-Garcia, R. Martinez-Exposito, M.L. Fernandez-de Cordova, E.J. Llorent-Martinez, Determination of the phenolic profile and antioxidant activity leaves and fruits of Spanish *Quercus coccifera*, J. Chem. 2018 (2018), https://doi.org/10.1155/2018/2573270.

[34] Y. Isobe, M. Arita, S. Matsueda, R. Iwamoto, T. Fujihara, H. Nakanishi, et al., Identification and structure determination of novel anti-inflammatory mediator resolvin E3, 17,18-dihydroxyeicosapentaenoic acid, J. Biol. Chem. 287 (13) (2012) 10525–10534, https://doi.org/10.1074/jbc.M112.340612.

[35] P.N. Mekam, S. Martini, J. Nguefack, D. Tagliazucchi, E. Stefani, Phenolic compounds profile of water and ethanol extracts of *Euphorbia hirta* L. leaves showing antioxidant and antifungal properties, South Afr. J. Bot. 127 (2019) 319–332, https://doi.org/10.1016/j.sajb.2019.11.001.

[36] E.J. Llorent-Martinez, S. Gouveia, P.C. Castilho, Analysis of phenolic compounds in leaves from endemic trees from Madeira Island. A contribution to the chemotaxonomy of Laurisilva forest species, Ind. Crops Prod. 64 (2015) 135–151, https://doi.org/10.1016/j.indcrop.2014.10.068.

[37] S. Ersan, O.G. Ustundag, R. Carle, R.M. Schweiggert, Identification of phenolic compounds in red and green pistachio (*Pistacia vera* L.) hulls (exo- and mesocarp) by HPLC-DAD-ESI-(HR)-MSn, J. Agric. Food Chem. 64 (26) (2016) 5334–5344, https://doi.org/10.1021/acs.jafc.6b01745.

[38] G.L. Chen, X. Li, F. Saleri, M.Q. Guo, Analysis of flavonoids in *Rhamnus davurica* and its antiproliferative activities, Molecules 21 (10) (2016), https://doi.org/10.3390/molecules21101275.

[39] A. Fathoni, E. Saepudin, A.H. Cahyana, D.U.C. Rahayu, J. Haib, Identification of Nonvolatile Compounds in Clove (*Syzygium Aromaticum*) from Manado. *2nd International Symposium On Current Progress In Mathematics And Sciences* (ISCPMS), Univ Indonesia, Fac Math & Nat Sci, Depok, 2016. INDONESIA.

[40] T. Beelders, D. de Beer, M.A. Stander, E. Joubert, Comprehensive phenolic profiling of *Cyclopia genistoides* (L.) vent. By LC-DAD-MS and -MS/MS reveals novel xanthone and benzophenone constituents, Molecules 19 (8) (2014) 11760–11790, https://doi.org/10.3390/molecules190811760.

[41] K. Lech, Universal analytical method for characterization of yellow and related natural dyes in liturgical vestments from Krakow, J. Cult. Herit. 46 (2020) 108–118, https://doi.org/10.1016/j.culher.2020.04.011.

[42] I. Nawrot-Hadzik, S. Slusarczyk, S. Granica, J. Hadzik, A. Matkowski, Phytochemical diversity in rhizomes of three reynoutria species and their antioxidant activity correlations elucidated by LC-ESI-MS/MS analysis, Molecules 24 (6) (2019), https://doi.org/10.3390/molecules24061136.

[43] T. Levandi, T. Pussa, M. Vaher, P. Toomik, M. Kaljurand, Oxidation products of free polyunsaturated fatty acids in wheat varieties, Eur. J. Lipid Sci. Technol. 111 (7) (2009) 715–722, https://doi.org/10.1002/ejlt.200800286.
[44] A. Patyra, M.K. Dudek, A.K. Kiss, LC-DAD-ESI-MS/MS and NMR analysis of conifer wood specialized metabolites, Cells 11 (20) (2022), https://doi.org/10.3390/cells11203332.
[45] M.D. Razola-Diaz, A.M. Gomez-Caravaca, E.J. Guerra-Hernandez, B. Garcia-Villanova, V. Verardo, New advances in the phenolic composition of tiger nut (*Cyperus esculentus* L.) by-products, Foods 11 (3) (2022), https://doi.org/10.3390/foods11030343.
[46] D. Perret, A. Gentili, S. Marchese, M. Sergi, L. Caporossi, Determination of free fatty acids in chocolate by liquid chromatography with tandem mass spectrometry, Rapid Commun. Mass Spectrom. 18 (17) (2004) 1989–1994, https://doi.org/10.1002/rcm.1582.
[47] G. Jerz, I. Skrjabin, R. Gök, P. Winterhalter, Anacardic Acid Profiling in Cashew Nuts by Direct Coupling of Preparative High-Speed Countercurrent Chromatography and Mass Spectrometry (prepHSCCC-ESI-/APCI-MS/MS). Recent Advances in the Analysis of Food and Flavors, ACS Symposium Series, 2012, pp. 145–165.
[48] S.G.B. Gowda, C.S. Liang, D. Gowda, F.J. Hou, K. Kawakami, S. Fukiya, et al., Identification of short-chain fatty acid esters of hydroxy fatty acids (SFAHFAs) in a murine model by nontargeted analysis using ultra-high-performance liquid chromatography/linear ion trap quadrupole-Orbitrap mass spectrometry, Rapid Commun. Mass Spectrom. 34 (17) (2020), https://doi.org/10.1002/rcm.8831.
[49] K. Urbanova, V. Vrkoslav, I. Valterova, M. Hakova, J. Cvacka, Structural characterization of wax esters by electron ionization mass spectrometry, J. Lipid Res. 53 (1) (2012) 204–213, https://doi.org/10.1194/jlr.D020834.
[50] N. Cardullo, V. Muccilli, R. Saletti, S. Giovando, C. Tringali, A mass spectrometry and H-1 NMR study of hypoglycemic and antioxidant principles from a *Castanea sativa* tannin employed in oenology, Food Chem. 268 (2018) 585–593, https://doi.org/10.1016/j.foodchem.2018.06.117.
[51] E. Cantos, J.C. Espin, C. Lopez-Bote, L. De la Hoz, J.A. Ordonez, F.A. Tomas-Barberan, Phenolic compounds and fatty acids from acorns (*Quercus* spp.), the main dietary constituent of free-ranged Iberian pigs, J. Agric. Food Chem. 51 (21) (2003) 6248–6255, https://doi.org/10.1021/jf030216v.
[52] M. Sud, E. Fahy, D. Cotter, A. Brown, E.A. Dennis, C.K. Glass, et al., LMSD: LIPID MAPS structure database, Nucleic Acids Res. 35 (2007) D527–D532, https://doi.org/10.1093/nar/gkl838.
[53] P.P. Kumar, R. Paramashivappa, P.J. Vithayathil, P.V.S. Rao, A.S. Rao, Process for isolation of cardanol from technical cashew (*Anacardium occidentale* L.) nut shell liquid, J. Agric. Food Chem. 50 (16) (2002) 4705–4708, https://doi.org/10.1021/jf020224w.
[54] F.H.A. Rodrigues, J.R.R. Souza, F.C.F. Franca, N. Ricardo, J.P.A. Feitosa, Thermal Oligomerisation of Cardanol, vol. 81, E-Polymers, 2006, https://doi.org/10.1515/epoly.2006.6.1.1027.
[55] S. Ravichandran, R.M. Bouldin, J. Kumar, R. Nagarajan, A renewable waste material for the synthesis of a novel non-halogenated flame retardant polymer, J. Clean. Prod. 19 (5) (2011) 454–458, https://doi.org/10.1016/j.jclepro.2010.09.010.
[56] S. Carroccio, P. Rizzarelli, C. Puglisi, G. Montaudo, MALDI investigation of photooxidation in aliphatic polyesters: poly(butylene succinate), Macromolecules 37 (17) (2004) 6576–6586, https://doi.org/10.1021/ma049633e.
[57] B. Ranby, Photodegradation and photo-oxidation of synthetic-polymers, J. Anal. Appl. Pyrolysis 15 (1989) 237–247, https://doi.org/10.1016/0165-2370(89)85037-5.